Direct Evidence for Confinement of Junctions to Lines in an 3 Miktoarm Star Terpolymer Microdomain Structure

Stella Sioula,[†] Nikos Hadjichristidis,[†] and Edwin L. Thomas*,[‡]

Department of Chemistry, University of Athens, Panepistimiopolis, 15771 Zografou, Athens, Greece, and Department of Materials Science, Massachusetts Institute of Technology, Cambridge, Massachusetts 02139

Received April 21, 1998
Revised Manuscript Received September 22, 1998

ABC miktoarm star terpolymers are molecules consisting of a central junction joining three arms of different composition. A new microdomain morphology with *p*6*mm* symmetry was discovered in miktoarm star terpolymers of polystyrene (PS), polyisoprene (PI), and poly(methyl methacrylate) (PMMA). The components microphase separate into a three-phase, two-dimensionally periodic microstructure having one-dimensionally continuous domains. The star molecular architecture gives the molecule the ability to chose which pairs of arm components arrange adjacently so as to minimize the unfavorable contact energies. Because the interfacial energy between the PI and PMMA microphases is quite large, the molecule adopts a novel microdomain structure, which completely avoids contact between these two components. The structure consists of triangular-prism-shaped PI domains; rectangular-prism-shaped PS domains and hexagonal cylinders of PMMA. Analysis of the microdomain geometry demonstrates that the star junction points reside on periodically spaced, parallel lines where all three types of microdomain interface intersect. Control of molecular architecture and composition points the way for the realization of new microdomain structures.

In the case of AB diblock copolymers, the composition, the segment-segment interaction parameter χ_{AB} and the total number of Kuhn segments ($N_A + N_B$) are the main parameters which determine the equilibrium microdomain structure primarily through the interplay of interfacial and chain deformation energies. The morphology of linear three component ABC triblock copolymers is governed by two independent composition variables (ϕ_A, ϕ_B, $\phi_C = 1 - \phi_A - \phi_B$) and by three interaction parameters (χ_{AB}, χ_{AC}, and χ_{BC}).[1,2] The other major factor influencing the microphase morphology is the sequence of the blocks in the linear chain.[3,4] Recent experimental[3−8] and theoretical[9,10] research on linear ABC block copolymers has demonstrated a very rich set of morphologies. In the case of an ABC three-miktoarm star terpolymer the microdomain morphology also depends on the same five independent parameters, but the star architecture eliminates block sequence as a factor. If the three arms in the star are chosen to have sufficiently large values of $(N_i + N_j)\chi_{ij}$ for all pairs, a microdomain structure comprised of nearly pure domains of each of the components will result. Furthermore, due to the macromolecular architecture, the star junction points will be restricted to lie on periodically spaced parallel lines (not necessarily straight) defined by the mutual intersection of the different domains. This situation is completely different from all previously-studied types of block copolymers, where the junctions between different blocks are uniformly distributed over the intermaterial dividing surface (IMDS) between the domains.[11]

The requirement to minimize interfacial boundary area (boundary length) at fixed volume (fixed area) favors the formation of constant mean curvature (CMC) domain boundaries in three (two) dimensions. In two dimensions the boundary structures are particularly simple, i.e., segments of circular arcs or straight lines. This preference for CMC microdomain structures is opposed by the tendency for the individual arms to form domains of optimal and uniform thickness so as to minimize chain deformation energy. The star architecture eliminates the possibility of one-dimensional periodic structures (lamellae). The two-dimensionally periodic structures in ABC miktoarm terpolymers will be comprised of polygonal partitionings in which all three components must contact at every vertex. The vertexes are the locations where the lines that contain the star junctions must pass. There are many possible three-dimensionally periodic microdomain structures, including parallel stacks of periodically space loops containing the star junctions.

Due to the considerable effort needed to prepare a well-defined ABC miktoarm star, only a few samples have been made. The first three-miktoarm stars were synthesized in 1992 by Iatrou and Hadjichristidis[12] and by Fujimoto et al.[13] Iatrou and Hadjichristidis synthesized stars comprised of arms of PS, 1,4-PI, and 1,4-polybutadiene (PB) whereas Fujimoto et al. made star terpolymers of PS, poly (dimethylsiloxane) (PDMS), and poly (*tert*-butyl methacrylate) (PtBMA). Recently Hückstädt et al.[14] prepared a three-miktoarm star of PS, 1,2-PB and PMMA, Sioula et al.[15] prepared stars of PS, 1,4-PI and PMMA, and Lambert et al. prepared 3 arm stars of PS, poly(ethylene oxide) with poly(ϵ-caprolactone) or PMMA or poly (1-lactide).[16] Morphological studies by the Hadjichristidis group[17] on the PS/PI/PB three-miktoarm star showed that the two dienes were mixed due to their low interaction parameter so the system only exhibited two types of microdomains. The morphology of the polymers originally prepared by Fujimoto et al.[13] was recently examined by Okamoto et al.[18] The PS/PDMS/PtBMA stars were found to microphase separate into three types of microdomains, as determined by DSC, TEM and SAXS. TEM results indicated the existence of some type of a regular microdomain structure with a 3-fold symmetry of the PMDS domains, but the other two microphase structures were not distinguished. The authors suggested all three microdomains to be continuous in three dimensions, but the data were insufficient for a specific microdomain model to be proposed.

We have recently examined the morphology of a series of three-miktoarm star terpolymers of PS, PI, and PMMA.[19] For three of the samples, the molecular weight of the PMMA block was systematically varied while those of the PS and PI blocks were held fixed. In the fourth sample, the PS and PMMA blocks were approximately of the same molecular weight while the

[†] University of Athens.
[‡] Massachusetts Institute of Technology.

10.1021/ma980622t CCC: $15.00
Published on Web 10/31/1998

Table 1. Molecular Characteristics of SIM Three-Miktoarm Star Terpolymers (SIM)[d]

polymer	M_w(PS)[a] ($\times 10^{-3}$)	M_w(PI)[a] ($\times 10^{-3}$)	M_w(SIM)[a] ($\times 10^{-3}$)	M_w/M_n[b]	PS/PI/PMMA (% wt)[c]	PS/PI/PMMA (% vol)	$\phi_A:\phi_B:\phi_C$	d_1^{SAXS} (Å)	$N_{SI}\chi_{SI}$	$N_{SM}\chi_{SM}$
SIM-72/77/109	72	77	258	1.12	28.5/29.6/41.9	28.8/34.1/37.1	1/1.2/1.3	706	93	30
SIM-92/60/94	92	60	247	1.12	37.2/24.3/38.5	37.8/28.1/34.1	1.3/1/1.2	636	90	31

[a] LALLS in THF at 25 °C. [b] SEC in THF at 30 °C. [c] ^{1}H NMR in $CDCl_3$ at 35 °C. PS content (% wt) determined from SEC−UV at 260 nm is 28.2 for SIM-72/77/109 and 37.0 for SIM-92/60/94, in good agreement with the NMR results and the calculated value from the M_w of the PS and the SIM (SIM-72/77/109; 27.9; SIM-92/60/94: 37.2). [d] The molecular weights of the PMMA arms were calculated from the molecular weights of PS, PI, and SIM. According to the literature[21] at 140 °C, $\chi_{SI} = 0.051$ and $\chi_{SM} = 0.017$ (we are unaware of any reported values of χ_{IM}). The interaction parameter between isoprene and methylmethacrylate should be considerably higher than the other pairs based on the difference in the relative solubility parameters ($\chi_{12} \sim (\delta_1 - \delta_2)^2$) so we expect $N_{IM}\chi_{IM}$ to exceed the value for $N_{SI}\chi_{SI}$ and $N_{SM}\chi_{SM}$ for both terpolymers.

PI arm was the majority component. All four of the samples exhibited a three-microphase two-dimensionally periodic microstructure of an inner PI column with a surrounding PS annulus in a matrix of PMMA. For two of the samples, the PI−PS and PS−PMMA interfaces were cylindrical, whereas for the other two samples, the PI−PS and PS−PMMA interfaces exhibited a unique nonconstant mean curvature (non-CMC) diamond-prism shape. In every case, the PS and PMMA blocks were partially mixed (the PMMA chain passed through the PS domain) in order to eliminate the highly unfavorable contact between the PI and PMMA blocks. Although it was expected that the junction points for such miktoarm stars would be constrained to lie on lines, the absence of periodic structures where all three domain types intersect implied that the junction points of the star molecules were actually distributed over the PS/PI IMDS as occurs for linear polymers. Two additional ABC miktoarm star samples have been made, which were much more nearly symmetric in the relative volume fractions of the blocks than the previous samples in order to promote the formation of new microdomain structures. Sample SIM-72/77/109 corresponds-to-a ratio of relative volume fractions of 1/1.2/1.3 and sample SIM-92/60/94 corresponds to 1.3/1/1.2.

High vacuum techniques, described elsewhere, were used for the anionic synthesis of the three-miktoarm star terpolymers.[15] size exclusion chromatography (SEC) was employed along with low-angle laser light scattering to characterize molecular weights. The composition of the polymers was analyzed by ^{1}H NMR, and the PS content was also determined by SEC−UV (see Table 1). Morphological characterization was principally by transmission electron microscopy (TEM). Approximately 0.7 mm thick films of the materials were cast from a dilute solution (∼4 wt %) in chloroform (solubility parameters: $CHCl_3$, $\delta = 9.3(cal/cm^3)^{1/2}$; PS, $\delta = 9.1(cal/cm^3)^{1/2}$; PI, $\delta = 8.2(cal/cm^3)^{1/2}$; PMMA, $\delta = 9.3(cal/cm^3)^{1/2}$). The films were then dried for 1 day under vacuum at room temperature and subsequently annealed under vacuum for 5 days at 140 °C. For TEM investigation, 500−1500 Å thick sections were cryomicrotomed at approximately −90 °C using a Reichert-Jung FC 4E cryoultramicrotome equipped with a diamond knife. Sections were picked up on 600-mesh copper grids and in order to enhance the mass−thickness contrast, they were placed in the vapors of a 4% osmium tetroxide− (OsO_4−) water solution for 1 h for selective staining of the PI phase or in the vapors of a 0.5% ruthenium tetroxide− (RuO_4−) water solution for half an hour for selective staining of the PS and PI phases. A JEOL 200CX electron microscope equipped with a double tilt goniometer stage was operated at 200 kV and at 100 kV in the bright field mode to examine the stained sections. X-ray diffraction patterns were acquired at room temperature on the Time-Resolved Diffraction Facility (station X12B) at the National Synchrotron Light Source at Brookhaven National Laboratory.[20]

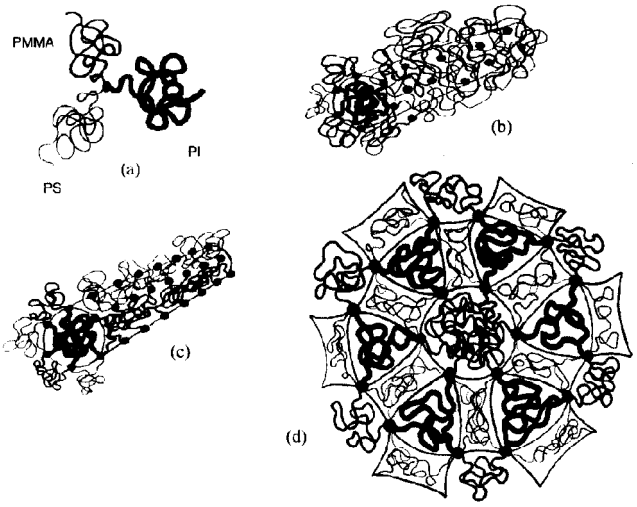

Figure 1. (a) Schematic of a miktoarm star molecule comprised of PS, PI and PMMA arms. (b−d) Proposed microdomain formation pathway. (b) The PI arms aggregate to form cylindrical micelles in a matrix of the PS and PMMA blocks and solvent. Star junctions are spread uniformly over the surface of the cylinder. (c) Further loss of solvent induces separation of PS and PMMA arms at the periphery of the cylinder. The star junctions become localized along lines tangent to the surface of the cylinder. (d) Self-assembly of the micellar units into a 2D hexagonal lattice occurs by match-up of the respective peripheral PS and PMMA regions of adjacent micelles. The PI regions deform into convex triangular prisms with the star junctions localized on lines passing through every vertex in the polygonal microdomain pattern.

The molecular characteristics of the three-miktoarm star terpolymers of styrene, isoprene, and methyl methacrylate (SIM) and the lowest order *d* spacings from the SAXS patterns are given in Table 1. The nomenclature used is SIM-*x*/*y*/*z* where *x*, *y*, *z* are the respective block molecular masses in kg/mol. TEM images of both terpolymer samples show a one-dimensionally periodic stripe pattern as well as two-dimensionally periodic patterns of domains depending on the viewing direction (see Figure 2). The overall domain order is limited with many defects and small grains. By careful tilting of the sections, regions with approximately 6-fold symmetry could be selected. Parts a and c of Figure 3 show a two-dimensional lattice of dark triangular shaped regions corresponding to the preferentially OsO_4-stained PI phase whereas the PS and PMMA phases are not distinguishable and appear as the light matrix. RuO_4-stained sections were also examined in order to distinguish between the PS and PMMA domains. In the RuO_4-stained micrographs (see Figure 3b and 3d), the

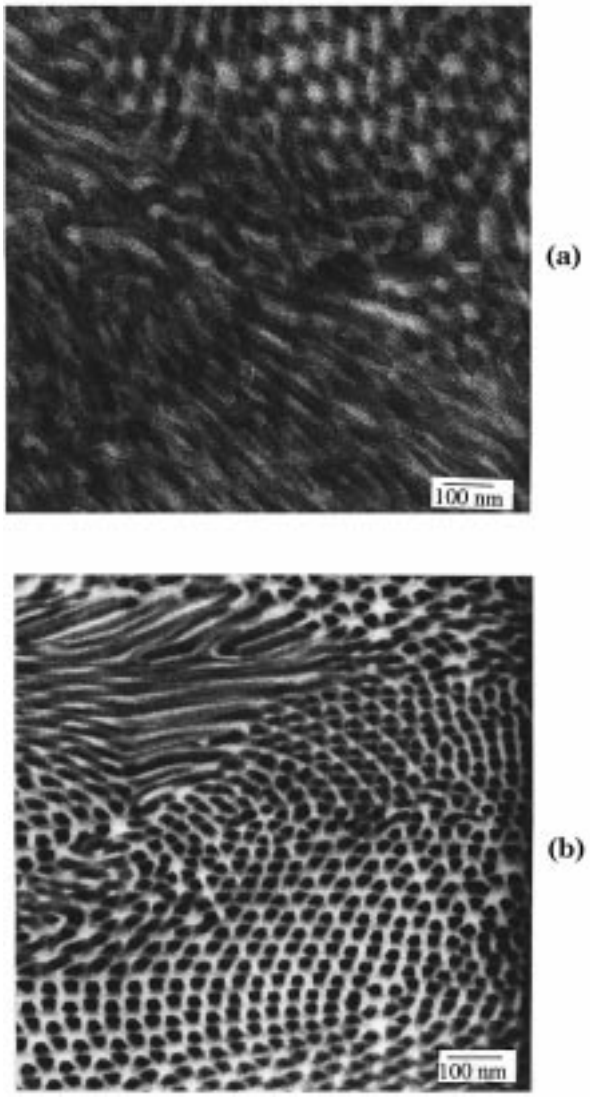

Figure 2. Bright field TEM micrographs (a) RuO_4-stained SIM-92/60/94 and (b) OsO_4-stained SIM-72/77/109. Note the stripe patterns and hexagonal patterns as well as the small grain size.

darkest regions correspond to the PI−PS interface, the gray regions to the PS and PI phases and the light regions to the PMMA phase. The gray-stained regions are seen to form a hexagonal mesh around light central regions. The most heavily stained regions are located at the nodes of the mesh.

As is evident from the micrographs, both samples SIM-92/60/94 and SIM-72/77/109 exhibit the same microdomain structure since even though the molecular weights are different, the volume fractions of each component are comparable. The approximate center-to-center distances between the PMMA domains (corresponding to the lattice parameter) determined from the TEM images are 900 and 1000 Å for the SIM-72/77/109 and SIM-92/60/94 samples, respectively. This is in reasonable agreement with the interdomain distances derived from the SAXS lattice parameters determined from the first broad peak assuming 2d hexagonal packing of the domains. From the TEM results it is obvious that there are no PI/PMMA interfaces, an occurrence we also observed in the other four SIM miktoarm star terpolymer samples.[18] This is accounted for by the relatively high degree of segregation (N_I + N_M)χ_{IM} for the isoprene and methyl methacrylate components (see Table 1).

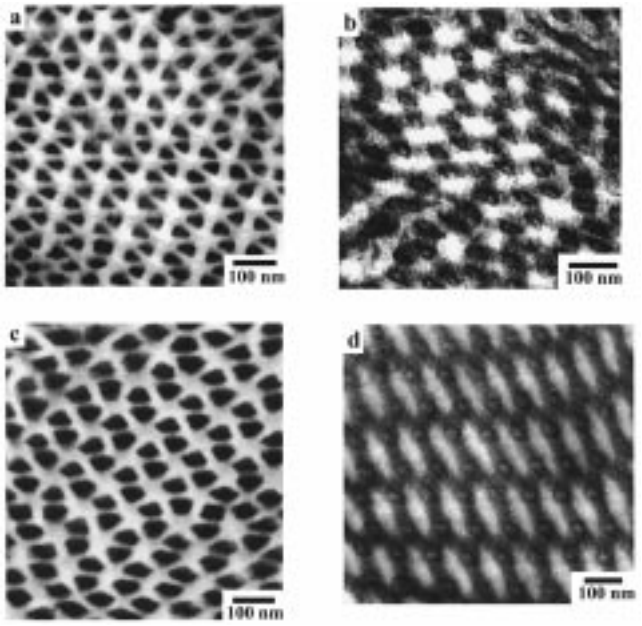

Figure 3. Bright field TEM images of selected regions viewing approximately along the one-dimensionally continuous axis of the structures: (a) SIM-92/60/94 stained with OsO_4; (b) SIM-92/60/94 stained with RuO_4; (c) SIM-72/77/109 stained with OsO_4; (d) SIM-72/77/109 stained with RuO_4. In the two OsO_4-stained micrographs, the dark regions correspond to the PI phase, which forms triangular prism-shape columns, whereas in the two RuO_4-stained micrographs, the dark regions correspond to the PI/PS phase boundary, the gray regions to the PS and PI phases, and the lightest regions to the PMMA phase.

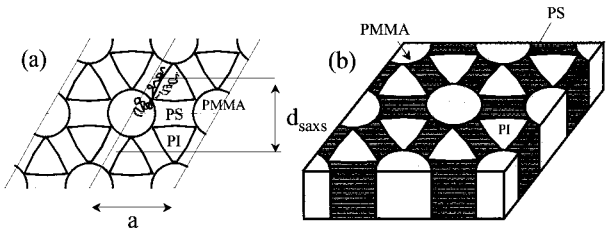

Plane group symmetry: p6mm

Figure 4. Schematics representing the proposed ABC miktoarm star microdomain structure. The areas of each component are proportional to the volume fractions for sample SIM-92/60/94. (a) Representative chain conformation of a three-arm star and the location of the junction point are indicated. The lattice parameter is a and the lowest order Bragg reflection corresponds to scattering from planes of spacing $d = \sqrt{3}\,a/2$. (b) Perspective showing the junction points residing at the vertexes where the three types of microdomains intersect.

A schematic representation of the microdomain structure based on the TEM and SAXS data is shown in Figure 4. In this drawing the area fractions of each component correspond approximately to the volume fractions of sample SIM-92/60/94. The PI phase forms convex triangular prism-shape columns centered on sites with 3-fold symmetry. The PI prisms connect to each other by PS columns forming a hexagonal mesh. The PS domains are centered on sites with 2-fold symmetry. These alternating PI and PS domains surround the PMMA phase, which forms hexagonal-shaped cylindrical columns on sites with 6-fold symmetry. The structure is two-dimensionally periodic with plane group

symmetry *p*6*mm*. Crystallographically, the PI domains are centered on Wyckoff site 2b, the PS domains on site 3c, and the PMMA domains on site 1a. All components form 1-dimensionally continuous domains. Interestingly, there is no matrix component.

Depending on the relative incompatibility of the various pairs of arms, there are three different pathways from the homogeneous state to the microphase-separated state. Additionally, the various component glass transitions and the inherent low mobility of high molecular weight star molecules hinder attainment of the global equilibrium structure. Whether a given polymer attains its global equilibrium structure in such systems with multiple microphase transitions is therefore problematic.

A possible scenario for the formation pathway of this structure is as follows (see Figure 1): Since chloroform is least preferential to the PI component, the first domains to form will be cylinders of PI in a swollen matrix consisting of PS, PMMA, and solvent. At this point, the star junctions are distributed uniformly over the cylindrical IMDS. Upon further solvent evaporation, the PS and PMMA arms will eventually segregate around the periphery of the PI cylinders. Due to the star architecture and comparable size of the PS and PMMA arms, one can imagine the formation of alternating zones of PS and PMMA around the PI core yielding PI cylinders with only 3m point group symmetry as a result of this peripheral segregation of the arms. These micellar-like units then self-assemble into the *p*6*mm* structure with the soft PI cores deforming into the triangular prisms as the strength of segregation increases with the continued loss of solvent. The junctions become localized along lines tangent to the PI prisms as the PS−PMMA interfaces become well-defined. The three PS domains that surround each PI domain virtually eliminate the higher energy interface between the PI and PMMA phases.

The data definitively shows that in these SIM stars the composition is favorable for a structure which allows the junction points to be confined to lines where the three different types of microdomains intersect. This feature is evident in the characteristic local singularities in interfacial curvature at the intersections of the three types of domains. The strongly inhomogeneous distribution of junctions over the IMDS has important implications for large strain deformation since the interfacial bonding between domains in these types of structures will consist primarily of noncovalent interactions.

Acknowledgment. This research was supported by the National Science Foundation through grant DMR 92-14853 and DMR 98-07591. S.S. and N.H. acknowledge the Greek General Secretariat of Research and Technology and the Research Committee of the University of Athens for support. E.L.T. also thanks K. Grosse-Brauckmann of the University of Bonn for useful discussions and the Center for Materials Science and Engineering at MIT for use of the electron microscope facility.

References and Notes

(1) Riess, G.; Schlienger, M.; Marti, S. *J. Macromol. Sci., Phys.* **1980**, *B17* (2), 335.
(2) Stadler, R.; Auschra, C.; Beckmann, J.; Krappe, U.; Voigt-Martin, I.; Leiber, L. *Macromolecules* **1995**, *28*, 3080.
(3) Gido, S. P.; Schwark, P. W.; Thomas, E. L.; Gonçales, M. C. *Macromolecules* **1993**, *26*, 2636.
(4) Mogi, Y.; Nomura, M.; Kotsuji, H.; Ohnishi, K.; Matsushita, Y.; Noda, I. *Macromolecules* **1994**, *27*, 6755.
(5) Auschra, C.; Stadler, R. *Macromolecules* **1993**, *26*, 2171.
(6) Junk, K.; Abetz, V.; Stadler, R. *Macromolecules* **1996**, *29*, 1076.
(7) Breiner, U.; Krappe, U.; Thomas, E. L.; Stadler, R.; Macromolecules **1998**, *31*, 135.
(8) Brinkmann, S.; Stadler, R.; Thomas, E. L. *Macromolecules* **1998**, *31*, 6566.
(9) Nakazawa, H.; Ohta, T. *Macromolecules* **1993**, *26*, 5503.
(10) Zheng, W.; Wang, Z.-G. *Macromolecules* **1995**, *28*, 7215.
(11) Thomas, E. L.; Anderson, D. M.; Henkee, C. S.; Hoffman, D.; Nature **1988**, *334*, 598.
(12) Iatrou, H.; Hadjichristidis, N. *Macromolecules* **1992**, *25*, 4649.
(13) Fujimoto, T.; Zhang, H.; Kazanawa, H.; Isono, X.; Hasegawa, H.; Hashimoto, T. *Polymer* **1992**, *33*, 2208.
(14) Hückstädt, H.; Abetz, V.; Stadler, R. *Macromol. Rapid Commun.* **1996**, *17*, 599.
(15) Sioula, S.; Tselikas, Y.; Hadjichristidis, N. *Macromolecules* **1997**, *30*, 1518.
(16) Lambert, O.; Reutenauer, S.; Hurtrez, G.; Reiss, G.; Dumas, P. *Polym. Bull.* **1998**, *40*, 143.
(17) Hadjichristidis, N.; Iatrou, H.; Behal, S. K.; Chludzinski, J. J.; Disko, M. M.; Garner, R. T.; Liang, K. S.; Lohse, D. J.; Milner, S. T. *Macromolecules* **1993**, *26*, 5812.
(18) Okamoto, S.; Hasegawa, H.; Hashimoto, T.; Fujimoto, T.; Zhang, H.; Kazama, T.; Takano, A. *Polymer* 1997, *38*, 5275.
(19) Sioula, S.; Hadjichristidis, N.; Thomas, E. L. *Macromolecules* **1998**, *31*, 5272.
(20) Capel, M. C.; Smith, G. C.; Yu, B. *Rev. Sci. Instrum.* **1995**, *66*, 2295.
(21) Balsara, N. P. Thermodynamics of Polymer Blends. Chapter 19 In *Physical Properties of Polymer Handbook*; Mark, J. E., Ed.; AIP Press: New York, 1996.

MA980622T